ONLINE FIRST September 9, 2026

Engineering Transactions, **74**, https://doi.org/10.24423/engtrans.2026.3574
Institute of Fundamental Technological Research Polish Academy of Sciences (IPPT PAN)
Université de Lorraine • Poznan University of Technology

Review Paper

Challenges of Corrosion, Wear, Erosion, and Abrasion in Hydropower Plants: Materials, Modeling, and Mitigation Strategies

Harvinder SINGH[1),2)]

[1)] *Department of Mechanical Engineering, Chandigarh Group of Colleges*
Landran, India

[2)] *Jadara University Research Center, Jadara University*
Irbid, Jordan

e-mail: honey.17aug@gmail.com

The chemical, food processing, hydropower, thermal power, and oil industries are among the sectors that frequently face problems of erosion, abrasion, and corrosion. Pipelines, elbows, reducers, separators, tees, and seals are among the hydraulic devices and pipeline components that are impacted by these phenomena. Silt erosion in turbines and related components is a major issue in hydropower plants, particularly in Indian hydropower plants where rivers contain hard minerals such as feldspar, quartz, and other mineral particles. Remarkably, high content of quartz in the silt causes problems in turbines, including sediment erosion, leakage, and secondary flow disturbances. Hydropower plants' total efficiency is ultimately jeopardized by these issues. This paper aims to support scholars and researchers by highlighting the following topics: (a) component failures in impulse and reaction turbines used in hydropower projects, (b) different turbine materials and their properties, and (c) a comparison of several thermal spraying techniques for turbine materials, along with numerous numerical models of erosion and abrasion informed by silt characteristics, material properties, and flow phenomena in different hydroturbines. The study also discusses modeling, pilot plant loops, wear mechanisms, and protective techniques aimed at mitigating wear and safeguarding hydroturbines.

Keywords: thermal spray coatings, erosion, component failure, turbine, hydropower plants.

Copyright © 2026 The Author(s).
Published by IPPT PAN. This work is licensed under the Creative Commons Attribution License CC BY 4.0 (https://creativecommons.org/licenses/by/4.0/).

1. Introduction

Global energy consumption is rising steadily, which is putting tremendous strain on all energy sources. Currently, the most widely used energy source comes from non-renewable fossil fuels. According to estimates, fossil fuel supplies could run out by the end of 21st century [1–3]. Fossil fuel burning also produces toxic

gaseous byproducts that harm the environment. These gases cause serious health hazards in addition to their contribution to climate change [4–7]. In response, renewable energy sources will soon be essential to meet our expanding energy needs. The basic understanding of using hydropower goes back to the mid-1770s, as demonstrated by the work of the French engineer Bernard Forest de Bélidor, who presented the working designs of horizontal and vertical hydraulic machinery [8–10]. However, the first hydropower-driven turbine came into existence in 1878 at Cragside in Northumberland, England, developed by William George Armstrong. Thereafter, the Schoelkopf power station in 1881 and the Edison hydroelectric power plant in 1882 in Appleton, Wisconsin, started to produce electricity from water[1)]. This was followed by rapid development, resulting in around 200 hydropower stations in the United States. alone by the end of 1889[2)]. A remarkable achievement was made in 1928 with the construction of Hoover Dam, with an initial capacity of 1345 MW. It remained the largest hydropower plant until 1936, when it was surpassed by the Grand Coulee dam in 1942[3)] with a capacity of 6809 MW. The trend to produce increasingly larger hydropower plants went on and in 1984, a plant with a capacity greater than 10 GW came into existence. The Itaipu Dam, a joint venture of Brazil and Paraguay with a capacity of 14 000 MW, was built. The construction of the Guri Dam in Venezuela with a capacity of 10 200 MW was initiated in 1963, and it is presently the third-largest dam in the world. The Three Gorges Dam in China, currently the largest hydroelectric power plant with a capacity of 22 500 MW, began operating in 2008[4)]. Today, China is the largest producer of hydroelectricity with 721 terawatt hours generated in 2010. Some countries, such as Norway, the Democratic Republic of Congo, Paraguay, and Brazil, are endowed with large water resources and have the potential to produce the bulk of their energy requirements through hydropower[3)]. Paraguay generates 100 % of its energy requirements from hydropower. It is also a source of national income, with 90 % of its electricity generation being exported to Brazil and Argentina. Norway also generates 98 % of its electricity needs from hydropower. At present, almost 16 % of the total generated energy in the entire world is from hydropower. This figure is expected to increase with the initiatives of Asian and African continents, where many of the hydropower resources remain unharnessed. In 2010, China alone added 16 GW of hydropower generation capacity and planned to add another 140 GW by 2015 [8–10].

In the current scenario, India is among the top ten hydroelectric power-generating countries. Out of its total installed capacity of 174 GW in 2012, 11 %

[1)] http://www.usbr.gov/power/edu/history.html
[2)] http://www1.eere.energy.gov
[3)] www.worldwatch.org
[4)] www.hydroworld.com

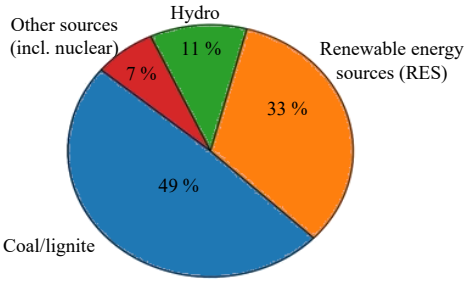

FIG. 1. Distribution of India's power generation capacity by energy source in 2012, RES stands for other renewable energy sources.

was contributed by the hydropower, as shown in Fig. 1. By the end of 2012, hydroelectric generation increased to 39 GW (an increase of ∼2 GW)[5)]. However, the percentage contribution of hydropower appears to have reduced marginally, as can be observed in Fig. 1. Nevertheless, the major projects currently under construction are surely expected to improve this figure. To mention a few, the hydropower plants at Upper Siang (11 000 MW), and Lower Subansiri (2000 MW) are some of the future projects that could help India gain significant momentum in the field of hydropower generation. In Fig. 2, the trend in hydroelectric generation with the total installed power generation capacity in India since 1950 can be found[5)]. It can be observed that hydropower has shown a steady and gradual rise since 1950. Indian rivers have a great potential for hydropower production, a significant portion of which remains untapped. Large potential lies in the Brahmaputra, Indus, and Ganga basins, which need to be developed. In terms

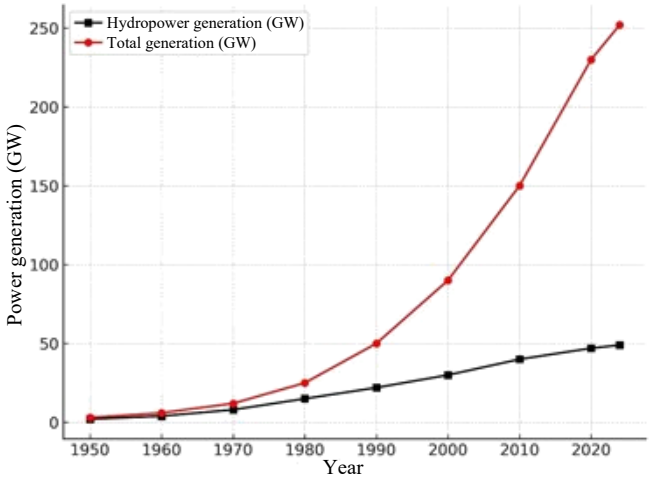

FIG. 2. Variation in India's hydropower and total power generation capacity from 1950 to 2024.

[5)] http://powermin.nic.in/

of installed hydroelectric generation capacity, India ranks sixth worldwide[3)]. An idea about the hydropower potential of India can be obtained from the fact that the country has a 150 000 MW hydropower capacity, which at a 60 % load factor amounts to around 84 000 MW. Additionally, 15 834 MW has been estimated from small hydropower projects. This provides an idea about the growth potential that can be expected in this sector [5].

2. Problems in hydropower plants

Ideally, a hydropower plant, once installed, should continue to operate without frequent breakdowns and problems. It is known that corrosion, a potential hazard for submerged turbines, is not a significant issue anymore in these plants. With the emergence of stainless steel in the early twentieth century, this material is widely used in hydraulic machinery where corrosion is a major concern. The addition of chromium (Cr) and nickel (Ni) to iron resulted in steels that are highly resistant to corrosion. With time, many different grades of stainless steels were developed by varying the proportions of their principal alloying elements, namely Cr and Ni. For hydroturbine applications, steels containing Cr $> 12\,\%$ are usually recommended [11, 12]. Various stainless steels that found their potential use in hydroturbine applications are listed in Table 1, along with their basic mechanical properties and microstructures. Among these different steels, 13Cr4Ni, also known by its trade name, CA6NM, is the most widely employed structural steel for hydroturbine applications. Here, the first letter C is a designation stating that it belongs to the corrosion-resistant family of stainless steels. The letter 'A' gives a rough estimation of the amounts of its major alloying elements. The numerals '6' represents 1/100th of the carbon content, which is 0.06 % in the present case. The last two letters are the representation of

Table 1. Properties of different turbine steels [21].

Stainless steel	Tensile strength [MPa]	Yield strength [MPa]	Elongation [%]	Impact strength [J]	Microstructure	Nature
13Cr1Ni	630	470	18	39	Martensite	Hard and brittle
13Cr6Ni	800	550	16	70	Martensite – 70 % Austenite – 30 %	–
17Cr4Ni	880	650	12	59	Martensite + Ferrite	Hard and ductile
13Cr4Ni	823	686	23	81	Martensite + Austenite	Hard
16Cr5Ni	880	600	21	100	Martensite – 65 % Austenite – 35 %	Hard and ductile

the alloying elements, namely Ni and Mo. The use of highly corrosion-resistant materials such as CA6NM has eliminated the problem of corrosion in hydroturbines. However, wear continues to affect the performance and degradation phenomenon of hydroturbines [13]. The performance of these hydroturbines is severely impacted by the presence of sand/silt particles in the river water that flows through the turbines [14–16]. Loosely bound soil particles, caused by deforestation, continue to be transported into rivers with rainwater. Secondly, the young mountains such as the Himalayas have fragile morphology; therefore, rivers originating from such mountain ranges experience a regular influx of sand, rocks, and debris due to frequent erosion and landslide activities [17–20].

3. Wear in hydroturbine

Wear is a surface degradation phenomenon resulting from the interaction of solid materials with the surrounding environment. As a result of wear, degradation at the surface of the material occurs either in the form of material loss or its relative displacement. Although it is a localized phenomenon at the initial stage, the damage to the material surface can intensify and coalesce upon continued exposure to degrading environments. This intensifies the degradation process, which further worsens the case and can result in the complete stalling of the system [21]. The accumulation of damage and the continuous loss of material from the surface can make the exposed component unfit for further service. Wear accounts for significant economic losses in any country. For example, according to an estimate given in 1965, the loss of 515 million pounds in the United Kingdom alone could have been avoided by giving due attention to tribology [22]. In Germany, the total losses due to wear in 1983 were estimated to be around 13 billion pounds. In the United States, losses due to friction have been estimated to be around $100 billion. Depending upon the type of the surrounding environment responsible for target surface wear and the material removal mechanism involved, the process of wear can be categorized into various types as discussed in the next section. Various types of wear mechanisms are presented in Fig. 3.

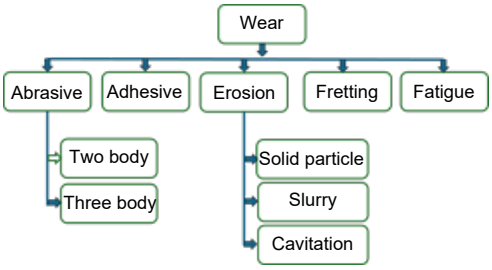

Fig. 3. Various types of wear mechanisms.

According to the American Society for Testing and Materials (see, ASTM-Standard G40, 2013), erosion is defined as the slow loss of original material from a solid surface that is produced by mechanical contact between the surface and a fluid, a multi-component fluid, or impinging liquid and/or solid particles. As it is clear from the definition itself, the impact of a fluid and/or solid, particles or both, results in mechanical damage of the surface, known as erosion. The different forms of erosion, shown in Fig. 4, can further help in understanding the different types of erosion. If erosion is brought on by the impact of solid particles that are entrained in a gaseous medium, this type of erosion is known as solid particle erosion (SPE). Slurry erosion (SE), on the other hand, is erosion that occurs when the liquid acts as a carrier medium rather than gas. Cavitation erosion (CE) and liquid droplet erosion (LDE) are two other types of erosion that arise generally from the interaction of the fluid and the solid surface. When CE is present, deterioration occurs because of cavitating circumstances that result from the implosion of cavities or bubbles within liquids containing vapor or mixtures of vapor and gas, as shown in Fig. 4. It was Rayleigh who first proposed that the collapse of vapor bubbles, resulting in very high loads. could initiate the phenomenon of cavitation [23].

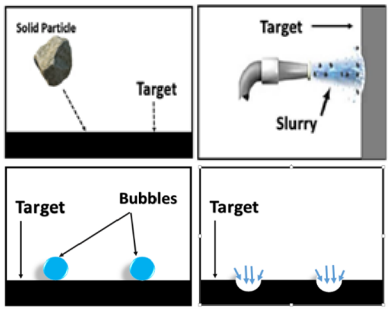

Fig. 4. Different types of erosion phenomena.

4. Impact of erosion on fluid machinery

There are several severely silt-affected hydropower stations in India. The categorization of these plants was made based on the level of impact energy possessed by the silt particles. Plants in which the particles had akinetic energy greater than 10 μJ required repair after every second monsoon, whereas repair was required after every three to four monsoons in the plants where the particle impact energy was in the range of 5 μJ to 10 μJ. The degraded blade of a 250 MW Francis turbine at Naptha Jhakri and Baira Siul [24] is shown in Fig. 5. Plants in which the impact energy of the particles was less than 5 μJ required repair after every seven to eight monsoons. In this categorization, however, no consideration was given to the concentration of the silt particles [24].

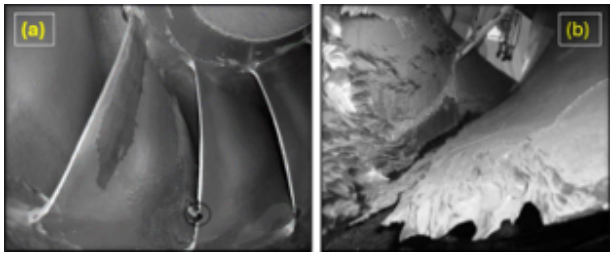

Fig. 5. Degraded turbine blade of a 250 MW Francis turbine at Naptha Jhakri and Baira Siul: a) degraded turbine blade, b) enlarged view of the degraded portion of the turbine blade.

5. Surface modification techniques

For the purpose of altering the surface characteristics of materials, a number of surface modification methods are shown in Fig. 6 [25, 26]. Some of these processes pose a threat to the environment [27, 28]. Two of such processes are chemical vapor deposition (CVD) and physical vapor deposition (PVD). Furthermore, using this method makes it challenging to create coatings that are thick. Additionally, the heat-affected zone (HAZ) that is generated during processing has an effect on the characteristics of the underlying substrate material in the form of dilution. Other methods, such as laser-assisted surface modification and weld overlay, are very closely related approaches. Thermal spraying is a versatile technique that can be used to deposit virtually any type of material onto almost any type of substrate material [**?**]. It is a versatile technique employing several combinations of materials to be coated onto substrates without significantly altering the properties of the substrate material. Another emerging technique for surface modification is friction stir processing (FSP) [29, 30].

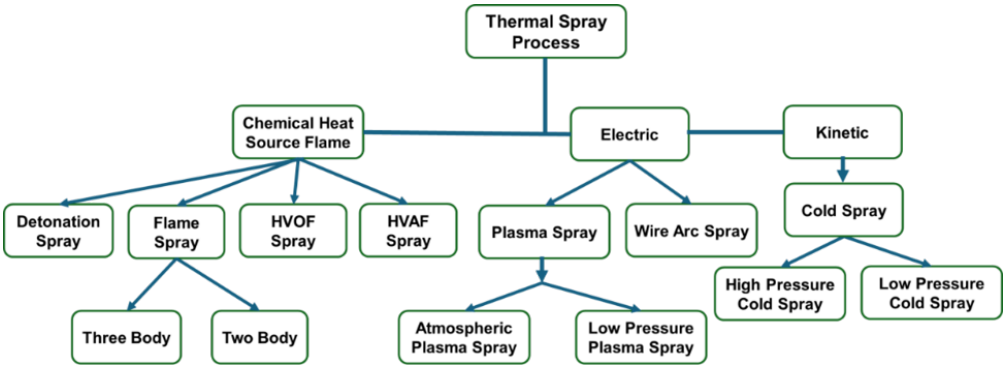

Fig. 6. Classification of thermal spray processes.

The thermal spraying technique involves spraying molten metal onto a substrate to deposit it as a coating. The coating material is first delivered as a pow-

der or wire, then heated to a molten state and next sprayed onto the substrate at high velocity, with particles as small as a micrometer. Thermal spraying uses combustion or an electrical arc discharge as the energy source. The material is covered by the sprayed particles as they accumulate on the substrate surface. The porosity, oxide content, macrohardness, surface roughness, and other characteristics of the coating affect its quality. Currently, these coatings are the most widely used. The use of highly erosion-resistant materials is restricted by financial and mechanical strength constraints. The cost of these materials is too high to present a practically viable solution. Secondly, known erosion resistant materials are typically hard and brittle; as a result, they are not able to resist the mechanical stresses induced during turbine operation. Given these facts, the most suitable option, which seems practically viable, is the use of surface modifications. Several surface modifications can be used to alter the surface properties of existing structural materials to resist degradation due to erosion, whereas the underlying structural material can continue to provide the required mechanical strength.

5.1. Plasma spraying process

It involves spraying the coating material onto the substrate surface in the form of a powder or wire while using a plasma torch to heat it to a high temperature. Placing the material in a plasma flame melts it and generates a high temperature. Next, this molten substance approaches the substrate. The substance quickly cools when it contacts the substrate, leaving an adhesive coating behind. Plasma gases, including argon, nitrogen, hydrogen, etc., flow via the anodic nozzle around the cathode. The plasma starts as a neutral flame, meaning it has no charge. The electric arc descends the nozzle once the plasma is prepared to spray. Because the cold gas of the anode nozzle is electrically non-conducting and increases the plasma arc's velocity, it constricts the plasma arc. The powder is heated quickly and propelled toward the substrate as it is fed into the plasma flame, creating an extremely strong and durable coating

5.2. Detonation spraying thermal spray coatings

The detonation gun, commonly known as the D-gun, is the main component of this process. A long, water-cooled barrel with an open end and a closed end makes up a D-gun. The coating material is delivered into the barrel together with oxygen and fuel gas, and this gas combination is ignited with a spark. The ensuing explosion warms and propels the powder into the barrel at supersonic speed. After every explosion, the barrel is additionally purged with a pulse of nitrogen. This procedure is repeated several times per second. The heated powder particles move toward the substrate's surface at a very fast speed of

roughly 600 m/s. Due to their fast speed, these particles have a high kinetic energy, which, when they collide with a substrate, creates an extremely thick and durable coating.

5.3. Wire arc spraying

During this thermal spraying procedure, two continuously fed metal wires are introduced into the spray gun. These wires are electrically charged, and an arc is created between them that melts the incoming wire tips. The air jet originating from the gun then carries the molten metal away. Wire arc spraying is the procedure by which this molten material is applied to the substrate. This type of coating is often used for thick coatings [31, 32].

5.4. Flame spraying

As part of this process, the fuel gas is burned in order to melt the spray coating material that is applied to the substrate. This fuel gas is often composed of acetylene or propane that has oxygen added to it. Wire or powder versions of the coating material are often used in the manufacturing process. The material is heated before being propelled onto the substrate to generate a surface coating.

5.5. High-velocity oxy-fuel (HVOF)

This coating process was developed during the 1980s. During this process, a combustion chamber is filled with a mixture of oxygen and fuel, which may be either gaseous or liquid. This mixture is continuously ignited, creating a steady flame. The heated gas that is produced then travels along a straight segment while being subjected to a pressure of one megapascal (MPa) via a nozzle that converges and diverges. The term 'fuel' may refer to either a liquid, such as kerosene, or a gas, such as hydrogen, methane, propane, or acetylene. The velocity of the exhaust jet emerging from the nozzle exceeds the local speed of sound, resulting in a supersonic gas stream. When injected into this gas stream, a powder feedstock has the potential to accelerate up to 800 m/s. The surface to be coated is approached and impinged by a stream of powder and hot gas at rapidly increasing temperatures. As the powder travels through the stream, it partially melts and then settles on the substrate. This particular coating has a low porosity and a high bond strength in contrast to other available coatings. There is a possibility that high-velocity oxy-fuel (HVOF) coatings, which are used for ceramic and metal coatings and are often utilized in operations to endure wear and corrosion, may be as thick as 12 mm. Tungsten carbide-cobalt (WC-Co), chromium carbide, alumina, and other powders are often used in the production of these coatings.

5.6. Cold spray (CS)

The cold spray (CS) method uses a De Laval nozzle with a convergent-divergent geometry to accelerate solid powder particles to supersonic velocities. Speeds between 300 m/s and 1200 m/s are used for the ballistic impingement of particles onto a suitable substrate. The parameters of the feedstock powders, in addition to the geometry of the nozzle, affect the ultimate temperature and velocity of the sprayed particles. These factors are directly connected to the microstructure of the coating, as well as its physical and mechanical attributes. The temperature of the gas stream never exceeds the point at which the feedstock material begins to melt. Because it is carried out in the solid state, this coating deposition method has characteristics that are quite different when compared to other standard thermal spray processes. There are now two primary types of cold spray systems: high-pressure cold spray (HPCS), which injects particles from a high-pressure gas source before the spray nozzle throat, and low-pressure cold spray (LPCS), which injects powder into the diverging region of the spray nozzle. Both of these cold spray methods are referred to as cold sprays. The particle speeds that LPCS devices can produce are limited to the range of 300 m/s to 600 m/s, and these devices are often portable and much smaller. They are used to apply light materials, and air or nitrogen that is readily available serves as their standard propellant gas. In systems with high pressure, we use particles with higher density. They typically generate particle velocities between 800 m/s and 1400 m/s, are stationary, and employ higher-pressure gases. Lighter gases such as nitrogen or helium are selected as the HPCS propellant gas [33].

6. Protection against erosion

6.1. Use of coatings

The damaging effects of erosion have been discussed in the preceding sections. In this part, we would like to elaborate on various protection schemes used for protection against degradation due to erosion. Erosion degradation can be reduced by either replacing the material with one that has greater erosion-resistant qualities, or by simply altering the surface of the components that are already in place. The drawback of the former approach is the high cost involved in replacing the material with a better one. Furthermore, property requirements may vary between the bulk and the surface. For instance, if the component were to be replaced with a harder material, it would reduce erosion. However, the component might lose certain mechanical properties, such as its toughness, ductility, and fracture resistance. With the use of the latter approach, however, we could certainly reduce cost and retain the desired bulk properties by modifying only the

surface properties to meet requirements. It has been shown that several emerging approaches for surface modification, such as cold spray, microwave-aided coatings, and friction stir processing, have demonstrated promising results and have the potential to replace some of the techniques currently in use.

6.2. Weld overlay technique

It was pointed out by Bonacorso *et al.* [34] that weld overlays are the most preferred technique for repairing eroded components of hydroturbines. However, the presence of complex geometries and unfavorable positions during repair poses difficulties for weld adhesion to the treated surface.

Wear studies on 2.5C2.7Cr and 6.7Cr weld overlays produced by gas metal arc welding (GMAW) having hardness of 550 HV and 650 HV were conducted by Dasgupta *et al.* [35]. It was observed that hard-faced steel performed better in comparison to the untreated steel specimens. A direct impact of the variation in the microstructure of the hard-faced overlays and steel on the erosion response and degrading mechanism was observed.

The slurry erosion of metal matrix composite (MMC) coatings developed using weld overlays was studied by Flores *et al.* [36]. Using the plasma transferred arc method, coatings comprising 65 wt.%WC in Fe-Cr-C matrixes were developed. The effect of this addition was evident in the microhardness values, which reached 1140 HV compared to 670 HV for the layer formed without any addition. Clearly, the MMC weld overlay showed more than a twofold improvement in erosion resistance at 20 °C, mainly ascribed to the presence of solid parts. Further extending his studies, Flores *et al.* [37] estimated the performance of a NiCrBSi matrix at high and low levels of alloying elements. Both matrixes were also reinforced with 65 wt.%WC. The NiCrBSi matrix containing higher alloying elements showed somewhat better erosion resistance than its counterpart. The addition of WC helped in improving the erosion performance by a factor of 4 to 5, however, somewhat better or slightly better performance was observed among the WC-reinforced matrixes.

Hattori and Mikami [38] evaluated the comparative behavior of cavitation erosion of Stellite 6 and 21 weld overlays against SS304 and SS316 using a cavitating jet and ultrasonic rigs. It was observed that Stellite overlays showed lower material losses (7- to 13-fold reduction) compared to SS304 steel. A direct correlation between erosion and hardness was observed.

Cavitation erosion tests of NOREM, D-CAV, CaviTec, and Hydroloy 914 advanced weld overlays deposited by GMAW showed erosion in the range of 1 mg/h to 2.6 mg/h, compared to 3.2 mg/h for SS308 [39]. However, the data presented does not lead to a direct comparison because of the different densities of these materials.

GMAW and SMAW weld overlays of Co-alloyed stainless-steel coatings showed a 12 times lower mass loss rate relative to SS316L when tested under cavitating conditions [40]. The mass loss rate was even lower than that of HVOF-coated Stellite 6 steel by a factor of 5. However, no direct correlation with hardness was noticed, showing a dependence on microstructure.

The problem of cavitation-corrosion erosion of a copper-manganese-aluminum (CAM) alloy during its service in marine conditions was presented by Li *et al.* [41]. It was found that the welded zone showed 4 times higher resistance in comparison to the base material. The HAZ showed a higher erosion response than the weld zone owing to a lack of phase transformation. The benefits of NiTi steel in a cavitating environment were discussed by Richman *et al.* [42]; however, its high cost and brittle behavior when formed into thick sections limit its practical usage. Two different alloys of NiTi (martensitic and austenitic) were explosively welded onto carbon steel at 0.56 mm to 0.68 mm thicknesses. The martensitic NiTi layers performed exceptionally well in comparison to their austenitic counterparts in the as-welded conditions. Heat treatment at 500 °C improved the response of the austenitic NiTi, showing a similar mass loss as to that of martensitic. Low-cycle fatigue showed a good correlation with the cavitation erosion behavior of various steels. A gas tungsten arc welding (GTAW) TiNi alloy subjected to slurry erosion studies showed a ductile response with maximum mass loss at a 30° impingement angle. An AISI 1048 alloy tested under similar conditions showed 50 % more mass loss at the highest level. This better performance was attributed to this alloy system's excellent work hardening and increased hardness, which resulted from the partial conversion of Ti into its oxides during the welding process [43]. Karimi *et al.* [44] studied the cavitation response of NiCrBSi-based weld overlays produced by the flame spray method. It was found that the presence of a uniformly distributed austenitic hard phase led to the highest erosion resistance of the Ni60B alloy, being even higher than that of austenitic stainless steel. Finally, CrMnB overlays were tested under cavitation-corrosion conditions owing to their better martensitic transformation capabilities, promoting work hardenability [45].

6.3. Thermal spray coatings

According to the literature, surface coatings may help such materials resist slurry erosion. Thermal spraying techniques have recently garnered a lot of interest among many coating deposition techniques. The CE behavior of thermal spray coatings, however, must be assessed [46–51].

Although WC-based thermal spray coatings may provide substantial slurry erosion resistance [52, 53], there is little information on their CE behavior. In [54], the performance of flame-sprayed WC/Co-FeNiCr and Cr_2O_3 coatings was examined and it was discovered that microstructural flaws such porosity and

partially or completely unmelted particles had an impact on this performance. Although these coatings demonstrated greater resistance to slurry erosion, they did not perform well when exposed to CE [55]. Even WC/Co and CrC coatings sprayed using HVOF sustained substantial damage under cavitating erosion conditions [55]. The CE resistance of the bare steel was not increased by other WC coatings. Conversely, FeCrSiBMn coatings applied via HVOF were tested and found to outperform uncoated ZG06Cr13Ni5Mo martensite stainless steel. The inclusion of complex carbides and increased hardness of the coatings were credited for improving resistance [56–59].

The literature also reveals that the slurry and CE behavior of Ni-Al_2O_3-based coatings has not been thoroughly studied. Recent research by Hu *et al.* [60] examined the effectiveness of cold-sprayed Ni + 40%Al_2O_3 coatings on Inconel-600 under slurry and CE [60]. They demonstrated that, despite the coating's improved slurry erosion performance, its CE performance was insufficient. The Ni component lower cavitation resistance and lower bonding strength were shown to be the main causes of coating deterioration. Additionally, the coating's microhardness was only 1.5 to 2.5 times greater than that of the substrate. Ahmed [61] discovered that contact fatigue loadings are mostly affected by the ratio of coating thickness to maximum shear stress depth. According to that research, this ratio has to be more than 1.5 for a longer operational lifespan [61].

NiTi has been shown to exhibit higher resistance against CE and wear, usually owing to its superelasticity and/or superplasticity properties [62–65]. It was reported that NiTi samples aged at 500 °C possessed 8.6 times higher resistance than those subjected to solution treatment [65]. However, the use of NiTi as a structural material is not a practically viable solution, owing to its high cost. Moreover, there could be a problem of brittleness in thick sections. Richman *et al.* [42] recommended applying the NiTi coating onto steel components using an explosive cladding technique to protect them against CE [42]. This led to a reduction in the erosion rates of low-carbon steel of the order of 30 times in comparison to SS304 steel. Other conventional coating routes, such as fusion welding or thermal spraying, are not well suited to this composition. During fusion reactions, brittle phases are introduced, and the stoichiometry of NiTi is also affected due to uncontrolled reactions [42]. Similarly, thermal-sprayed NiTi coatings often exhibit low adherence to steel and lack the structural integrity to make them resistible against CE [66, 67]. Although around nine times higher CE resistance of NiTi coatings produced via tungsten inert gas (TIG) against that of SS316 steel has been reported [68], this resistance was still significantly lower in comparison to that of solution heat-treated NiTi bulk alloys. This low resistance of NiTi coating in comparison to bulk NiTi alloy was observed despite the high hardness of the former, which could be due to the loss of superelasticity during the coating process. Thermal-sprayed NiTi coatings also did not

show any further improvement due to the presence of pores acting as structural defects. Furthermore, the reaction of the feedstock powders with the surrounding environment (O_2 and N_2) results in the formation of brittle phases that eventually lead to the loss of erosion resistance [69]. Furthermore, variations in erosion rates with a Ni content in the coating was also reported, where coatings containing a Ni content higher than the equiatomic ratio showed higher resistance. After reviewing the relevant literature, it was discovered that a substantial amount of research has not yet beenconducted to assess the performance of NiTi alloys and coatings with regard to slurry erosion and/or slurry erosion-corrosion [70].

6.4. Ni-alumina-based coatings

Luo *et al.* [71] evaluated the toughness and strength of the Ni-Al_2O_3 composites prepared using hot isostatic pressing (HIP) with Ni contents varying from 0 % to 30 %. When the amount of nickel in the composite increased, it was discovered that the strength of the composite decreased, while its structure toughness rose [72]. The maximum hardness reported was 175 HV1.0 for the composite coating containing 45 vol.% of the hard phase, whereas the coating with 40 vol.% Al_2O_3 exhibited the maximum hardness of around 650 HK0.1. This variance in hardness was ascribed to the average size of the reinforcing particles (coatings containing much smaller particles around 1 μm in size), along with a large grain size in the composite on the order of 1 mm. Moreover, the microhardness also increased to 524 HV with a rise in alumina content. Similar results have also been reported in [73, 74]. Szczygieł and Kołodziej [75] also deposited Ni-6%Al_2O_3 coatings using an electrochemical deposition route and evaluated their corrosion performance. Furthermore, different coatings were investigated by several researchers [76, 79–83] to determine their microstructure and characteristics. Table 2 provides a review of the various coating materials used to combat erosion.

The coating was found to be successful in enhancing the slurry erosion resistance of Inconel 600. Li *et al.* [77] showed the feasibility of depositing Ni-Al_2O_3 coatings containing a large volume fraction of hard-phase constituents using a cold spray technique [76]. The maximum microhardness obtained was only around 173 ±33 HV0.2, whereas the hardness of the pure Ni coating was found to be around 131 HV0.2. Turunen *et al.* [78] deposited nanocrystalline $NiAl_2O$. Recently, various researchers have employed distinct thermal spray coatings to combat corrosion, erosion, and other degradation mechanisms in different sectors, such as thermal power generation, hydroelectric power, gas turbines, aerospace engineering and others. Thus, thermal spray coatings have significant potential in the coming future.

TABLE 2. Summary of past research carried out on different coating materials for combating erosion [85–112].

No.	Reference	Coating materials	Substrate	Process	Coating thickness [µm]	Average particles size [µm]	Applications	Remarks/findings
1	[85]	Ni-SiC	SS316L	Microwave cladding	500–600	40 ±5	Hydropower plant	– Ni cladding without SiC powder showed a hardness of 360 HV. – The Ni-10 wt.% SiC cladding yielded the highest CE resistance and optimal mechanical results.
2	[86]	Ni and Ni-Inconel 718 powder	Duplex stainless steel	Cold spray	Up to 3000	16–45		– Achieved a 215 HV hardness with the Ni-Inconel 718 coatings. – Observed an 80 % reduction in overall mass loss and higher CE resistance due to the addition of Inconel 718.
3	[87]	WOKA-3653 (86WC-10Co-4Cr)	AISI 410	HVOF	227	11–45		– Demonstrated a high slurry erosion resistance. – Tungsten carbide coatings exhibited a 50 % lower erosion rate at an impact angle of 30°.

Table 2. [Cont.]

No.	Reference	Coating materials	Substrate	Process	Coating thickness [μm]	Average particles size [μm]	Applications	Remarks/findings
4	[88]	WC-10Co-4Cr powder	SS 316	HVOF	302	25–40	Hydropower plant	– The modified PTFE shows high hardness varying from 255 to 290 HV. – Due to its high hardness, it has a better slurry erosion resistance.
5	[89]	Iron-based amorphous powder (SHS 574)	AISI 316	HVOF	180–200	15–53		– Observed lower erosive wear rate at impact angles of 30° and 45°. – Observed a higher erosive wear rate at 90°.
6	[90]	Ni-40TiO_2 Ni-20TiO_2-20Al_2O_3	13Cr4Ni	HVAF	422 ±10 354 ±10	10–40		– Found lower porosity in the range of 0.8 % to 3.6 % for nanostructured composite coatings. – Found higher porosity in the Ni-20TiO_2-20Al_2O_3 coating than the Ni-40TiO_2 coating.
7	[91]	B4C KBF4 SiC	13Cr-4Ni	Pack boronizing method	40	–		– Found higher erosive wear resistance of the 13-4 martensitic stainless steel (MSS) compared to bare steel substrate due to coating high hardness (2300 VHN).

Table 2. [Cont.]

No.	Reference	Coating materials	Substrate	Process	Coating thickness [μm]	Average particles size [μm]	Applications	Remarks/findings
8	[92]	Ni-Cr-40Al_2O_3	SS316L	HVFS	500–600	50–70 60–90 35–60	Hydropower plant	– The microhardness of the Ni-Cr-40Al_2O_3 coating was 225 HV; however, after processing coatings it increased 2 times and increased fracture toughness.
9	[93]	Ni60 and WC-17Co	17-4PH stainless steel	APPS and HVOF	238–416	140–325 mesh 350–500 mesh		– Volume loss was lowered by 50.6 % compared to the substrate material. WC-17Co is the best coating material for water droplet erosion (WDE) resistance.
10	[94]	Ni+20%Cr7C3	CA6NM	Microwave cladding	920–1010	100–150		– Observed high erosion resistance, it was found that the average weight loss reduced by 45 % in clad samples compared to CA6NM.
11	[95]	WC-10Co-4Cr	AISI 410 stainless steel	HVOF	112–155	11–45		– Improved the wear properties and high hardness (278 HV) were achieved with low coating porosity of 0.3 % to 0.7 % of the deposited coatings.

Table 2. [Cont.]

No.	Reference	Coating materials	Substrate	Process	Coating thickness [μm]	Average particles size [μm]	Applications	Remarks/findings
12	[96]	Cr_3C_2-20(80Ni20Cr) WC-Ni	ANSI 1018	HVOF	221 ±16 118 ±8	10–45 15–45	Turbine steel	– Observed a 20.5 % improvement in hardness, i.e., increasing from 846 HV to 1020 HV. – Observed the lowest porosity of about 1 % for Cr_3Cr_2-NiCr cermet coatings.
		Cr_3C_2-25NiCr WC-17Co WC-12Co WC-10Co-4Cr Cr_3C_2-40NiCr	1.4571 high-alloyed-steel	HVOF	100–200	20–40		
		Conventional WC-12Co Nanostructured WC-12Co CeO_2 modified WC-12Co	Stainless steel AISI 304	HVOF	–	15–45 5–45 15–45		
		WC-CoCr Cr_3C_2-NiCr Al_2O_3	S355 steel		163 176 294	15–45 15–45 5–22		
		WC-10Cr-4Co	1Cr18Ni9Ti stainless steel	HVOF HVAF	380–420	16–45 5–30		
		Cr_3C_2-NiCr Ni-Cr-Fe	1018 steel	APS	200 150	10–90		
13	[97]	Cr_3C_2+25NiCr	13Cr4Ni	Plasma spraying	220 ±15	15–45		– Achieved coating micro–hardness values up to 1050 VHN coatings. – Decreased cumulative mass loss compared to the bare reference steel.

Table 2. [Cont.]

No.	Reference	Coating materials	Substrate	Process	Coating thickness [μm]	Average particles size [μm]	Applications	Remarks/findings
14	[98]	TiAlN coatings	AA1050 AA5083	HVOF	105–150	2–50 2–70	Hydropower plant	– Observed erosion at 160 g/min, 195 g/min, and 265 g/min at impingement angles of 75°, 60°, and 30°, respectively.
15	[99]	Al_2O_3-13%TiO_2 and Cr_3C_2-25NiCr	CA6NM	D-gun	–	5–30 15–45		– Found lower erosion in Cr_3C_2-25NiCr coating than the Al_2O_3-13%TiO_2. – Observed cumulative weight loss range from 0.1 mg to 1.5 mg in Cr_3C_2-25NiCr coating compared to 3.5 mg to 8.5 mg in Al_2O_3-13%TiO_2 coating.
16	[100]	WC-CoCr	SS410	HVAF HVOF	380–420	1.2		– Found excellent hardness, fracture toughness, and surface residual stress in WC-Co-Cr coatings.
17	[101]	86WC-10Co4Cr	SS410	HVOF HVAF	410	16–45 20–45		– Achieved hardness value up to 1473 HV0.3 with lower porosity (0.3 % to 0.9 %). – Observed lower weight loss due to cavitation.
18	[102]	Al 6061 powder	ASTM C633	HPCS	2000–8000	5–68	Al-6061 hydraulic valve actuator	– Recorded an increase in hardness accompanied by low porosity varying from 0.93 % to 1.66 %.

Table 2. [Cont.]

No.	Reference	Coating materials	Substrate	Process	Coating thickness [μm]	Average particles size [μm]	Applications	Remarks/findings
19	[103]	WC-Co-Cr and Ni-Cr-B-Si	13Cr-4Ni	Plasma thermal spray	250–400	5–50	Hydropower plant	– Mass loss increases with increasing particle in velocity. – Recorded cumulative mass loss at 15 mg/cm^2, 12 mg/cm^2, 25 mg/cm^2 in WC-Co-Cr, Ni-Cr-B-Si coatings and for bare steel, respectively.
20	[104]	Stellite-6 and Cr_3C_2-25Ni4Cr	13Cr-4Ni	D-gun	100–150	10–53 10–45		– Observed overall specific weight loss of 1897.43 g/m^2 and 345.31 g/m^2 in 13Cr4Ni and Stellite-6 coatings, respectively, after a 6-hour test run. – Observed a 5.5 times higher specific weight loss in 13Cr4Ni than in the Stellite-6.
21	[105]	Ni-Al_2O_3	CA6NM	HVFS	24–684	20–100 20–60	Turbine steel	– Recorded high erosion resistance for coatings containing 40 wt.% alumina. Uncoated steel showed a 2.2 higher erosion rate.

Table 2. [Cont.]

No.	Reference	Coating materials	Substrate	Process	Coating thickness [μm]	Average particles size [μm]	Applications	Remarks/findings
22	[106]	WC-10Co-4Cr	CF8M turbine steel	D-gun	200	15–45	Turbine steel	– Found a reduction in the erosion rate of WC-10Co-4Cr coatings. – Achieved high hardness of 1120 HV with low porosity of 1 %.
23	[107]	WC-10Co-4Cr and Al_2O_3+13TiO_2	CF8M turbine steel	HVOF	830–1160	15–45 10–45		– Found high erosion resistance in WC-10Co-4Cr coatings compared to the Al_2O_3+13TiO_2.
24	[108]	Wallex-50 and Tribaloy-700 powders	16Cr-5Ni	Laser surface alloying	600–1000	200	Hydropower plant	– Found excellent ductility and superior impact toughness even at low temperatures.
25	[109]	Co-based Stellite 6 powders and Ni-based Colmonoy 88	13Cr-4Ni steel	Laser surface alloying (LSA)	300–400	100		– Observed a 1.250 to 2-fold improvement in hardness relative to the base substrate material.
26	[110]	Ti-6Al-4V 17Cr-4Ni PH Steel 12Cr steel	ASTM G73-98	HVOF	250 ±30	5–50	Steam turbine blades	– Achieved high surface hardness and a low erosion rate with HVOF coating.
27	[111]	WC-12Co Cr_3C_2+25NiCr	13Cr-4Ni and T410	D-gun	50–250	5–45	Turbine components	– Concluded that the degradation rate of hard coatings depends upon the erodent particle size and total concentration.
28	[112]	Ni-Cr-B-Si composite coating, WC+Ni-Cr-B-Si	Stainless steel 18-8	Plasma spraying process	500 ±5	5–50	Hydropower plant	– Reached a peak surface hardness of 1150 HV along with a 0.73 mg/10h CE.

7. Conclusions

Hydroelectric power plants in the Himalayan region and other high-sediment mountainous environments face persistent hydro-abrasive erosion, affecting nearly 40 % of installations worldwide. This review synthesizes three decades of multidisciplinary research into a unified framework for understanding and mitigating silt-induced turbine degradation, highlighting that erosion severity is governed by the combined effects of suspended sediment characteristics, hydraulic operating conditions, and turbine material properties. Field observations indicate that unprotected CA6NM components can suffer erosion rates of 0.5 mm to 3 mm per year, with trailing-edge damage exceeding tip erosion by three to four times. Over time, three complementary mitigation strategies have emerged, including upstream sediment management, advanced protective coatings, and computational fluid dynamics (CFD)-based turbine design optimization, each offering measurable reductions in erosion and associated maintenance costs. Despite these advances, significant research gaps remain, including large site-to-site variability in erosion calibration despite IEC 62364:2019 standardization, limited understanding of coating durability under transient and seasonal operating conditions, insufficient studies on Kaplan turbine erosion in run-of-river schemes, early-stage integration of real-time monitoring with machine-learning-based prediction, and the absence of comprehensive life-cycle assessments comparing mitigation pathways. Available evidence shows that integrated approaches combining moderate sediment reduction, design optimization, and selective coating application can reduce material loss by 40 % to 60 %, lower overall costs by 25 % to 35 %, and extend maintenance intervals by 2 to 3 times. Implementing sediment-aware operational strategies, real-time monitoring, site-specific erosion assessment, cost-optimized coatings, and upstream sediment control can collectively reduce erosion losses by 30 % to 50 %, thereby extending component lifespans from 3–7 years to 12–20 years, and significantly enhancing the long-term sustainability of hydropower systems worldwide.

7.1. Future research directives

Future research directives derived from this study are as follows:

- investigate and optimize thermal spraying techniques (air plasma, D-gun, cold spraying, HVOF) to improve the erosion-corrosion resistance of hydroturbine blade steels,
- focus on processing methods to achieve defect-free thermal spray coatings, thereby minimizing porosity, micro-cracks, through-pores, and enhancing coating hardness,

- research rare earth and nanostructured powder materials to optimize coating material combinations for improved performance in hydroturbine applications,
- study the incorporation of solid lubricants in thermal spray coatings to assess their impact on wear reduction and friction, ensuring cost-effectiveness for specific applications,
- investigate the effects of post-spray heat treatment on the microstructure and bond strength of thermal spray coatings to enhance their corrosion and wear resistance,
- research techniques to further harden thermal spray coatings and reduce their porosity to increase erosion resistance in practical applications.

The abovementioned research directives highlight key areas for future exploration and development in improving thermal spray coatings for hydropower applications.

Fundings

This research did not receive any specific grant from funding agencies in the public, commercial, or not-for-profit sectors.

Conflict of interest

The author declares that there are no known competing financial interests or personal relationships that could have influenced the work described in this paper.

Authors' contributions

The author conceptualized the study, performed the analysis, wrote the original draft, and approved the final manuscript.

References

1. Oerlikon, https://www.oerlikon.com.
2. Kranzler T., Ensuring product quality through customized materials tests: Classification of materials, *Sulzer Technical Review*, 2010, https://www.sulzer.com/-/media/files/about-us/our-company/innovation/str_2010_1_e_11_kraenzler_e.pdf?sc_lang=en.
3. Sangal S., Singhal M.K., Saini R.P., Hydro-abrasive erosion in hydro turbines: a review, *International Journal of Green Energy*, **15**(4): 232–253, 2018, https://doi.org/10.1080/15435075.2018.1431546.
4. Ministry of Power, Government of India, https://powermin.gov.in.
5. National Hydroelectric Power Corporation, https://www.nhpcindia.com.

6. Bedi T.S., Kumar S., Kumar R., Corrosion performance of hydroxyapatite and hydroxyapatite/titania bond coating for biomedical applications, *Materials Research Express*, **7**(1): 015402, 2020, https://doi.org/10.1088/2053-1591/ab5cc5.
7. Kumar S., Kumar M., Handa A., Combating hot corrosion of boiler tubes: a study, *Engineering Failure Analysis*, **94**: 379–395, 2018, https://doi.org/10.1016/j.engfailanal.2018.08.004.
8. Alam T., Islam M.A., Farhat Z.N., Slurry erosion of pipeline steel: effect of velocity and microstructure, *Journal of Tribology*, **138**(2): 021604, 2016, https://doi.org/10.1115/1.4031599.
9. Manisekaran T., Kamaraj M., Shariff S.M., Joshi S.V., Slurry erosion studies on surface-modified 13Cr-4Ni steels: effect of angle of impingement and particle size, *Journal of Materials Engineering and Performance*, **16**(5): 567–572, 2007, https://doi.org/10.1007/s11665-007-9068-5.
10. Bonsor K., How Hydropower Plants Work, HowStuffWorks.com, n.d., https://science.howstuffworks.com/environmental/energy/hydropower-plant1.html.
11. Bitter J.G.A., A study of erosion phenomena: Part II, *Wear*, **6**(3): 169–190, 1963, https://doi.org/10.1016/0043-1648(63)90073-5.
12. Singh H., Kumar M., Singh R., Development of high-pressure cold spray coatings of tungsten carbide composites, *Materials Today: Proceedings*, **116**: 21–28, 2023, https://doi.org/10.1016/j.matpr.2022.12.210.
13. Singh H., Kumar M., Singh R., Microstructural and mechanical characterization of a cold-sprayed WC-12Co composite coating on stainless steel hydroturbine blades, *Journal of Thermal Spray Technology*, **32**: 970–983, 2022, https://doi.org/10.1007/s11666-022-01497-8.
14. Singh H., Kumar M., Singh R., An overview of various applications of cold spray coating process, *Materials Today: Proceedings*, **56**(Part 5): 2826–2830, 2022, https://doi.org/10.1016/j.matpr.2021.10.160.
15. Kumar S., Kumar M., Jindal N., Overview of cold spray coatings applications and comparisons: a critical review, *World Journal of Engineering*, **17**(1): 27–51, 2020, https://doi.org/10.1108/WJE-01-2019-0021.
16. Franc J.P., Michel J.M. [Eds], *Fundamentals of Cavitation*, Kluwer Academic Publishers, Dordrecht, 2004.
17. Santa J.F., Baena J.C., Toro A., Slurry erosion of thermal spray coatings and stainless steels for hydraulic machinery, *Wear*, **263**(1–6): 258–264, 2007, https://doi.org/10.1016/j.wear.2006.12.061.
18. Chauhan A.K., Goel D.B., Prakash S., Erosion behaviour of hydro turbine steels, *Bulletin of Materials Science*, **31**(2): 115–120, 2008, https://doi.org/10.1007/s12034-008-0020-6.
19. Amarendra H.J., Chaudhari G.P., Nath S., Synergy of cavitation and slurry erosion in the slurry pot tester, *Wear*, **290–291**: 25–31, 2012, https://doi.org/10.1016/j.wear.2012.05.025.
20. Romo S.A., Santa J.F., Giraldo J.E., Toro A., Cavitation and high-velocity slurry erosion resistance of welded Stellite 6 alloy, *Tribology International*, **47**: 16–24, 2012, https://doi.org/10.1016/j.triboint.2011.10.003.

21. Singh H., Kumar M., Singh R., Combating slurry and cavitation erosion of hydro turbine blades: a study, *International Journal of Advanced Science and Technology*, **29**: 5744–5755, 2020.

22. Singh H., Singh M., Singh R., A comprehensive review of erosion behaviour of hydro turbine blades and their remedies by HVOF process, *Journal of Critical Reviews*, **7**(19): 1738–1746, 2020.

23. Singh H., Khosla H., Sidhu T.S., Kalsi S.B.S., Karthikeyan J., Characteristic study of N07718 superalloy surface prepared by cold spray, *Materials and Manufacturing Processes*, **33**(2): 140–148, 2018, https://doi.org/10.1080/10426914.2016.1269922.

24. Singh H., Khosla H., Walia G.S., Sidhu T.S., Kalsi S.B.S., Karthikeyan J., Characteristic study of cold sprayed N06601 superalloy surface, *Surface Engineering*, **34**(5): 369–379, 2018, https://doi.org/10.1080/02670844.2017.1312220.

25. Pauleau Y. [Ed.], *Materials Surface Processing by Directed Energy Techniques*, Elsevier, Oxford, 2006.

26. Pawlowski L., *The Science and Engineering of Thermal Spray Coatings*, 1st ed., John Wiley & Sons, Chichester, 1995.

27. Young M.A., Health hazards of electroplating, *Journal of Occupational Medicine*, **7**(7): 348–352, 1965.

28. Koropchak J.A., Roychowdhury S.B., Evidence for aerosol ionic redistribution within aerosols produced by chrome electroplating, *Environmental Science & Technology*, **24**(12): 1861–1863, 1990, https://doi.org/10.1021/es00082a012.

29. Mishra R.S., Ma Z.Y., Friction stir welding and processing, *Materials Science and Engineering: R: Reports*, **50**(1–2): 1–78, 2005, https://doi.org/10.1016/j.mser.2005.07.001.

30. Kumar R., Kumar S., Thermal spray coating process: a study, *International Journal of Engineering Sciences and Research Technology*, **7**(3): 610–617, 2018, https://doi.org/10.5281/zenodo.1207005.

31. Kumar K., Kumar S., Gill H.S., Role of surface modification techniques to prevent failure of components subjected to the fireside of boilers, *Journal of Failure Analysis and Prevention*, **23**: 1–5, 2023, https://doi.org/10.1007/s11668-022-01556-w.

32. Kumar S., Kumar M., Tribological and mechanical performance of coatings on piston to avoid failure – a review, *Journal of Failure Analysis and Prevention*, **22**(5): 1346–1369, 2022, https://doi.org/10.1007/s11668-022-01436-3.

33. Bregliozzi G., Di Schino A., Haefke H., Kenny J.M., Cavitation erosion resistance of a high nitrogen austenitic stainless steel as a function of its grain size, *Journal of Materials Science Letters*, **22**(14): 981–983, 2003, https://doi.org/10.1023/A:1024673215823.

34. Bonacorso N., Gonçalves Jr. A., Dutra J.C., Automation of the processes of surface measurement and of deposition by welding for the recovery of rotors of large-scale hydraulic turbines, *Journal of Materials Processing Technology*, **179**(1–3): 231–238, 2006, https://doi.org/10.1016/j.jmatprotec.2006.03.081.

35. Dasgupta R., Prasad B.K., Jha A.K., Modi O.P., Das S., Yegneswaran A.H., Slurry erosive wear characteristics of a hard-faced steel: effect of experimental parameters, *Wear*, **213**(1–2): 41–46, 1997, https://doi.org/10.1016/S0043-1648(97)00181-6.

36. Flores J.F., Neville A., Kapur N., Gnanavelu A., An experimental study of the erosion–corrosion behavior of plasma transferred arc MMCs, *Wear*, **267**(1–4): 213–220, 2009, https://doi.org/10.1016/j.wear.2008.11.015.

37. Flores J.F., Neville A., Kapur N., Gnanavelu A., Erosion–corrosion degradation mechanisms of Fe–Cr–C and WC–Fe–Cr–C PTA overlays in concentrated slurries, *Wear*, **267**(11): 1811–1820, 2009, https://doi.org/10.1016/j.wear.2009.02.005.

38. Hattori S., Mikami N., Cavitation erosion resistance of stellite alloy weld overlays, *Wear*, **267**(11): 1954–1960, 2009, https://doi.org/10.1016/j.wear.2009.05.007.

39. Kumar A., Boy J., Zatorski R., Stephenson L.D., Thermal spray and weld repair alloys for the repair of cavitation damage in turbines and pumps: a technical note, *Journal of Thermal Spray Technology*, **14**(2): 177–182, 2005, https://doi.org/10.1361/10599630523737.

40. Boccanera L., Barra S.R., Buschinelli A.J.A., Schwetzke R., Kreye H., Cavitation erosion resistance of Co-alloyed stainless steel weld claddings as compared to thermal sprayed coatings, [in:] *Proceedings of XXV Encontro Nacional de Tecnologia da Soldagem*, Belo Horizonte, Brazil, 1999.

41. Li X., Yan Y., Ma L., Xu Z., Li J., Cavitation erosion and corrosion behaviour of copper–manganese–aluminum alloy weldment, *Materials Science and Engineering: A*, **382**(1–2): 82–89, 2004, https://doi.org/10.1016/j.msea.2004.04.032.

42. Richman R.H., Rao A.S., Kung D., Cavitation erosion of NiTi explosively welded to steel, *Wear*, **181–183**(Part 1): 80–85, 1995, https://doi.org/10.1016/0043-1648(95)90011-X.

43. Weng J.R., Chang J.T., Chen K.C., Le J.L., Solid/liquid erosion behaviour of gas tungsten arc welded TiNi overlay, *Wear*, **255**(1–6): 219–224, 2003, https://doi.org/10.1016/S0043-1648(03)00120-0.

44. Karimi M.R., Salimijazi H.R., Golozar M.A., Effects of remelting processes on porosity of NiCrBSi flame sprayed coatings, *Surface Engineering*, **32**(3): 238–243, 2016, https://doi.org/10.1179/1743294415Y.0000000107.

45. Zheng Y., Luo S., Ke W., Cavitation erosion–corrosion behaviour of CrMnB stainless overlay and 0Cr13Ni5Mo stainless steel in 0.5 M NaCl and 0.5 M HCl solutions, *Tribology International*, **41**(12): 1181–1189, 2008, https://doi.org/10.1016/j.triboint.2008.02.011.

46. Cheng F.T., Kwok C.T., Man H.C., Laser surfacing of S31603 stainless steel with engineering ceramics for cavitation erosion resistance, *Surface and Coatings Technology*, **139**(1): 14–24, 2001, https://doi.org/10.1016/S0257-8972(00)01103-8.

47. Tam K.F., Cheng F.T., Man H.C., Cavitation erosion behavior of laser-clad Ni–Cr–Fe–WC on brass, *Materials Research Bulletin*, **37**(7): 1341–1351, 2002, https://doi.org/10.1016/S0025-5408(02)00766-3.

48. Lo K.H., Cheng F.T., Kwok C.T., Man H.C., Improvement of cavitation erosion resistance of AISI 316 stainless steel by laser surface alloying using WC powder, *Surface and Coatings Technology*, **165**(2–3): 258–267, 2003, https://doi.org/10.1016/S0257-8972(02)00739-9.

49. Duraiselvam M., Galun R., Wesling V., Mordike B.L., Reiter R., Oligmüller J., Cavitation erosion resistance of AISI 420 martensitic stainless steel laser-clad

with nickel aluminide intermetallic composites and matrix composites with TiC reinforcement, *Surface and Coatings Technology*, **201**(3–4): 1289–1295, https://doi.org/10.1016/j.surfcoat.2006.01.054.

50. Duraiselvam M., Galun R., Siegmann S., Wesling V., Mordike B.L., Liquid impact erosion characteristics of martensitic stainless steel laser clad with Ni-based intermetallic composites and matrix composites, *Wear*, **262**(3–4): 279–286, 2007, https://doi.org/10.1016/j.wear.2006.03.024.

51. Duraiselvam M., Galun R., Wesling V., Mordike B.L., Reiter R., Oligmüller J., Buvanashekaran G., Cavitation erosion resistance of Ti6Al4V laser alloyed with TiC-reinforced composites, *Materials Science and Engineering: A*, **454–455**: 63–68, 2007, https://doi.org/10.1016/j.msea.2006.11.002.

52. Mann B.S., Arya V., An experimental study to corelate water jet impingement erosion resistance and properties of metallic materials and coatings, *Wear*, **253**(5–6): 650–661, 2002, https://doi.org/10.1016/S0043-1648(02)00118-7.

53. Grewal H.S., Bhandari S., Singh H., Parametric study of slurry-erosion of hydroturbine steels with and without detonation gun spray coatings using Taguchi technique, *Metallurgical and Materials Transactions A*, **43**(9): 3387–3401, 2012, https://doi.org/10.1007/s11661-012-1174-5.

54. Singh H., Kumar S., Kumar R., Chauhan J.S., Impact of operating parameters on electric discharge machining of cobalt-based alloys, *Materials Today: Proceedings*, 2023, https://doi.org/10.1016/j.matpr.2023.01.234.

55. Santa J.F., Espitia L.A., Blanco J.A., Romo S.A., Toro A., Slurry and cavitation erosion resistance of thermal spray coatings, *Wear*, **267**(1–4): 160–167, 2009, https://doi.org/10.1016/j.wear.2009.01.018.

56. Oka Y.I., Miyata H., Erosion behaviour of ceramic materials caused by water droplet impingement, *Wear*, **267**(11): 1804–1810, 2009, https://doi.org/10.1016/j.wear.2009.02.009.

57. Sang K., Li Y., Cavitation erosion of flame spray weld coating of nickel-base alloy powder, *Wear*, **189**(1–2): 20–24, 1995, https://doi.org/10.1016/0043-1648(95)06608-X.

58. Kumar S., Handa A., Chawla V., Grover N.K., Kumar R., Performance of thermal-sprayed coatings to combat hot corrosion of coal-fired boiler tube and effect of process parameters and post-coating heat treatment on coating performance: a review, *Surface Engineering*, **37**(7): 833–860, 2021, https://doi.org/10.1080/02670844.2021.1924506.

59. Wang Y., Li P., Cheng C., Wang Z., Cheng M., Huan J., Cavitation erosion characteristics of a Fe–Cr–Si–B–Mn coating fabricated by high velocity oxy-fuel (HVOF) thermal spray, *Materials Letters*, **61**(8–9): 1867–1872, 2007, https://doi.org/10.1016/j.matlet.2006.07.147.

60. Hu H.X., Jiang S.L., Tao Y.S., Xiong T.Y., Zheng Y.G., Cavitation erosion and jet impingement erosion mechanism of cold-sprayed Ni–Al_2O_3 coating, *Nuclear Engineering and Design*, **241**(12): 4929–4937, 2011, https://doi.org/10.1016/j.nucengdes.2011.09.038.

61. Ahmed R., Contact fatigue failure modes of HVOF coatings, *Wear*, **253**(3–4): 473–487, 2002, https://doi.org/10.1016/S0043-1648(02)00163-1.

62. Shida Y., Sugimoto Y., Water jet erosion behaviour of Ti–Ni binary alloys, *Wear*, **146**(2): 219–228, 1991, https://doi.org/10.1016/0043-1648(91)90064-2.

63. Richman R.H., Rao A.S., Hodgson D.E., Cavitation erosion of two NiTi alloys, *Wear*, **157**(2): 401–407, 1992, https://doi.org/10.1016/0043-1648(92)90076-K.

64. Wu S.K., Lin H.C., Yeh C.H., A comparison of the cavitation erosion resistance of TiNi alloys, SUS304 stainless steel and Ni-based self-fluxing alloy, *Wear*, **244**(1–2): 85–93, 2000, https://doi.org/10.1016/S0043-1648(00)00443-9.

65. Cheng F.T., Shi P., Man H.C., Correlation of cavitation erosion resistance with indentation-derived properties for a NiTi alloy, *Scripta Materialia*, **45**(9): 1083–1089, 2001, https://doi.org/10.1016/S1359-6462(01)01143-5.

66. Jardine A.P., Field Y., Herman H., Marantz D.R., Kowalsky K.A., Processing and properties of arc-sprayed shape memory effect NiTi, *Scripta Metallurgica et Materialia*, **24**(12): 2390–2396, 1990, https://doi.org/10.1016/0956-716X(90)90099-3.

67. Jardine P., Field Y., Herman H., Shape memory effect in vacuum plasma sprayed NiTi, *Journal of Materials Science Letters*, **10**(16): 943–945, 1991, https://doi.org/10.1007/BF00719963.

68. Cheng F.T., Lo K.H., Man H.C., NiTi cladding on stainless steel by TIG surfacing process: Part I. Cavitation erosion behavior, *Surface and Coatings Technology*, **172**(2–3): 308–315, 2003, https://doi.org/10.1016/S0257-8972(03)00345-1.

69. Zhou K.S., Wang D.Z., Liu M., A study of the cavitation erosion behaviour of a Ti-Ni alloy coating, *Surface and Coatings Technology*, **34**(1): 79–87, 1988, https://doi.org/10.1016/0257-8972(88)90091-6.

70. Hiraga H., Inoue T., Shimura H., Matsunawa A., Cavitation erosion mechanism of NiTi coatings made by laser plasma hybrid spraying, *Wear*, **231**(2): 272–278, 1999, https://doi.org/10.1016/S0043-1648(99)00133-7.

71. Luo F., Xue H., Zhu D., W., Mechanical and dielectric properties of Ni/Al_2O_3 composites [in Chinese], *Transactions of Nonferrous Metals Society of China*, **17**(Suppl. 1): S1140–S1143, 2007.

72. Levin B.F., DuPont J.N., Marder A.R., The effect of second phase volume fraction on the erosion resistance of metal-matrix composites, *Wear*, **238**(2): 160–167, 2000, https://doi.org/10.1016/S0043-1648(99)00363-4.

73. Tian R., Cheng Y.F., Electrolytic deposition of Ni–Co–Al_2O_3 composite coating for erosion resistance, *Electrochimica Acta*, **53**(2): 511–517, 2007, https://doi.org/10.1016/j.electacta.2007.07.013.

74. Wu G., Li N., Zhou D., Mitsuo K., Electrodeposited Co–Ni–Al_2O_3 composite coatings, *Surface and Coatings Technology*, **176**(2): 157–164, 2004, https://doi.org/10.1016/S0257-8972(03)00739-4.

75. Szczygieł B., Kołodziej M., Composite Ni/Al_2O_3 coatings and their corrosion resistance, *Electrochimica Acta*, **50**(20): 4188–4195, 2005, https://doi.org/10.1016/j.electacta.2005.01.040.

76. Hu H.X., Jiang S.L., Tao Y.S., Xiong T.Y., Zheng Y.G., Cavitation erosion and jet impingement erosion mechanism of cold sprayed Ni–Al_2O_3 coating, *Nuclear Engineering and Design*, **241**(12): 4929–4937, 2011, https://doi.org/10.1016/j.nucengdes.2011.09.038.

77. Li W., Zhang C., Liao H., Li J., Coddet C., Characterizations of cold-sprayed Nickel–Alumina composite coating with relatively large Nickel-coated Alumina powder, *Surface and Coatings Technology*, **202**(19): 4855–4860, 2008, https://doi.org/10.1016/j.surfcoat.2008.04.076.

78. Turunen E., C T., Gustafsson T.E., Keskinen J., Fält T., Hannula S.P., Parameter optimization of HVOF sprayed alumina composite coatings, *Surface and Coatings Technology*, **200**(16–17): 4987–4994, 2006, https://doi.org/10.1016/j.surfcoat.2005.05.018.

79. Hou Q.Y., Huang Z., Wang J.T., Influence of nano-Al_2O_3 particles on the microstructure and wear resistance of the nickel-based alloy coating deposited by plasma transferred arc overlay welding, *Surface and Coatings Technology*, **205**(9–10): 2806–2812, 2011, https://doi.org/10.1016/j.surfcoat.2010.10.047.

80. Guan H., Xiao H., Ouyang S., Tang A., Chen X., Tan J., Feng B., She J., Zheng K., Pan F., A review of the design, processes, and properties of Mg-based composites, *Nanotechnology Reviews*, **11**(1): 712–730, 2022, https://doi.org/10.1515/ntrev-2022-0043.

81. Yang G.R., Song W.M., Lu J.J., Hao Y., Ma Y., Three-point bending behavior of surface composite Al_2O_3/Ni on bronze substrate produced by vacuum infiltration casting, *Journal of Materials Processing Technology*, **202**(1–3): 195–200, 2008, https://doi.org/10.1016/j.jmatprotec.2007.08.066.

82. Feng J., Ferreira M.G.S., Vilar R., Laser cladding of Ni–Cr/Al_2O_3 composite coatings on AISI 304 stainless steel, *Surface and Coatings Technology*, **88**(1–3): 212–218, 1997, https://doi.org/10.1016/S0257-8972(96)02909-X.

83. Feng Q., Li T., Teng H., Zhang X., Zhang Y., Liu C., Jin J., Investigation on the corrosion and oxidation resistance of Ni-Al_2O_3 nano-composite coatings prepared by sediment co-deposition, *Metal Finishing*, **107**(1): 34–41, 2009, https://doi.org/10.1016/S0026-0576(09)80007-X.

84. Feng Q., Li T., Zhang Z., Zhang J., Liu M., Jin J., Preparation of nanostructured Ni/Al_2O_3 composite coatings in high magnetic field, *Surface and Coatings Technology*, **201**(14): 6247–6252, https://doi.org/10.1016/j.surfcoat.2006.11.019.

85. Babu S., Arora H.S., Singh H., Grewal H.S., Microwave synthesized composite claddings with enhanced cavitation resistance, *Wear*, **422–423**: 242–251, 2019, https://doi.org/10.1016/j.wear.2019.01.072.

86. Kazasidis M., Yin S., Cassidy J., Volkov-Husović T., Vlahović M., Martinović S., Kyriakopoulou E., Lupoi R., Microstructure and cavitation erosion performance of nickel–Inconel 718 composite coatings produced with cold spray, *Surface and Coatings Technology*, **382**: 125195, 2020, https://doi.org/10.1016/j.surfcoat.2019.125195.

87. Thakur L., Arora N., A comparative study on slurry and dry erosion behaviour of HVOF sprayed WC–CoCr coatings, *Wear*, **303**(1–2): 405–411, 2019, https://doi.org/10.1016/j.wear.2013.03.028.

88. Bansal A., Singh J., Singh H., Slurry erosion behavior of HVOF-sprayed WC-10Co-4Cr coated SS 316 steel with and without PTFE modification, *Journal of Thermal Spray Technology*, **28**: 1448–1465, 2019, https://doi.org/10.1007/s11666-019-00903-y.

89. Vignesh S., Balasubramanian V., Sridhar K., Thirumalaikumarasamy D., Slurry erosion behavior of amorphous coating, *Metallography, Microstructure, and Analysis*, **8**: 462–471, 2019, https://doi.org/10.1007/s13632-019-00552-1.

90. Sharma V., Kaur M., Bhandari S., Development and characterization of high-velocity flame sprayed Ni/TiO_2/Al_2O_3 coatings on hydro turbine steel, *Journal of Thermal Spray Technology*, **28**(7): 1379–1401, 2019, https://doi.org/10.1007/s11666-019-00918-5.

91. Nath G., Kumar S., Slurry erosion behaviour of pack boronized 13-4 martensitic stainless steel for hydro turbine blades, *Materials Today: Proceedings*, **5**(9): 17380–17388, 2018, https://doi.org/10.1016/j.matpr.2018.04.151.

92. Rani M., Perumal G., Roy M., Grewal H.S., Singh H., Arora H.S., Post-processing of Ni–Cr–Al_2O_3 thermal spray coatings through friction stir processing for enhanced erosion–corrosion performance, *Journal of Thermal Spray Technology*, **28**(7): 1466–1477, 2019, https://doi.org/10.1007/s11666-019-00891-z.

93. Zhang Z., Zhang D., Xie Y., Experimental study on water droplet erosion resistance of coatings (Ni60 and WC-17Co) sprayed by APS and HVOF, *Wear*, **432–433**: 202950, 2019, https://doi.org/10.1016/j.wear.2019.202950.

94. Singh B., Zafar S., Effect of microwave exposure on slurry erosion behavior of Ni + 20% Cr_7C_3 composite clads, *Wear*, **426–427**(Part A): 491–500, 2019, https://doi.org/10.1016/j.wear.2018.12.016.

95. Ludwig G.A., Malfatti C.F., Schroeder R.M., WC10Co4Cr coatings deposited by HVOF on martensitic stainless steel for use in hydraulic turbines: resistance to corrosion and slurry erosion, *Surface and Coatings Technology*, **377**: 124918, 2019, https://doi.org/10.1016/j.surfcoat.2019.124918.

96. Tiwari A., Seman S., Singh G., Jayaganthan R., Nanocrystalline cermet coatings for erosion–corrosion protection, *Coatings*, **9**(6): 400, 2019, https://doi.org/10.3390/coatings9060400.

97. Kaushal S., Singh S., Slurry erosion behavior of plasma sprayed coatings, *Industrial Lubrication and Tribology*, **71**(1): 1–9, 2019, https://doi.org/10.1108/ILT-07-2016-0155.

98. Kiragi V.R., Patnaik A., Singh T., Fekete G., Parametric optimization of erosive wear response of TiAlN-coated aluminium alloy using Taguchi method, *Journal of Materials Engineering and Performance*, **28**(2): 838–851, 2019, https://doi.org/10.1007/s11665-019-03901-4.

99. Dev D.K., Erosion behaviour of hydroturbine material under air jet erosion tester using D-GUN coating, [in:] *2018 IEEE International Conference on Smart Energy Grid Engineering (SEGE)*, pp. 321–324, 2018, https://doi.org/10.1109/SEGE.2018.8499445.

100. Kumar R.K., Kamaraj M., Seetharamu S., Pramod T., Sampathkumaran P., Effect of spray particle velocity on cavitation erosion resistance characteristics of HVOF and HVAF processed 86WC-10Co4Cr hydro turbine coatings, *Journal of Thermal Spray Technology*, **25**(5): 1217–1230, 2016, https://doi.org/10.1007/s11666-016-0427-3.

101. Kumar R.K., Kamaraj M., Seetharamu S., Anand Kumar S., A pragmatic approach and quantitative assessment of silt erosion characteristics of HVOF and HVAF processed WC-CoCr coatings and 16Cr5Ni steel for hydro turbine applications, *Materials & Design*, **132**: 79–95, 2017, https://doi.org/10.1016/j.matdes.2017.06.046.

102. Singh H., Kumar S., Kumar R., Chohan J.S., Impact of operating parameters on electric discharge machining of cobalt-based alloys, *Materials Today: Proceedings*, 2023, https://doi.org/10.1016/j.matpr.2023.01.234.

103. Goyal D.K., Singh H., Kumar H., Sahni V., Slurry erosion behaviour of HVOF sprayed WC–10Co–4Cr and Al_2O_3+13TiO_2 coatings on a turbine steel, *Wear*, **289**: 46–57, 2012, https://doi.org/10.1016/j.wear.2012.04.016.

104. Singh H., Bhandari S., Slurry erosion behavior of thermal sprayed coatings, *International Journal of Research in Mechanical Engineering Technology*, **3**(2): 201–206, 2013.

105. Grewal S., Agrawal A., Singh H., Slurry erosion performance of Ni–Al_2O_3 coatings, *Tribology International*, **66**: 296–306, 2013, https://doi.org/10.1016/j.triboint.2013.06.010.

106. Bhandari S., Singh H., Kumar H., Rastogi V., Slurry erosion performance of detonation gun sprayed coatings, *Journal of Thermal Spray Technology*, **21**(5): 1054–1065, 2012, https://doi.org/10.1007/s11666-012-9799-1.

107. Goyal D.K., Singh H., Kumar H., Sahni V., Slurry erosion behaviour of HVOF sprayed WC–10Co–4Cr and Al_2O_3+13TiO_2 coatings on a turbine steel, *Wear*, **289**: 46–57, 2012, https://doi.org/10.1016/j.wear.2012.04.016.

108. Sathik S., Periasamy V.M., Kamaraj M., Shariff S.M., Improvement of slurry erosion wear resistance of 16Cr-5Ni martensite stainless steel by LSA and LTH, *Journal of Materials Engineering and Performance*, **22**(12): 3689–3698, 2013, https://doi.org/10.1007/s11665-013-0678-9 .

109. Shivamurthy R.C., Kamaraj M., Nagarajan R., Shariff S.M., Padmanabham G., Influence of microstructure on slurry erosive wear characteristics of laser surface alloyed 13Cr–4Ni steel, *Wear*, **267**(1–4): 204–212, 2009, https://doi.org/10.1016/j.wear.2008.12.027.

110. Mann B.S., Arya V., HVOF coating and surface treatment for enhancing droplet erosion resistance of steam turbine blades, *Wear*, **254**(7–8): 652–667, 2003, https://doi.org/10.1016/S0043-1648(03)00253-9.

111. Mann B.S., High-energy particle impact wear resistance of hard coatings and their application in hydroturbines, *Wear*, **237**(1): 140–146, 2000, https://doi.org/10.1016/S0043-1648(99)00310-5.

112. Mann B.S., Krishnamoorthy P.R., Vivekananda P., Cavitation erosion characteristics of nickel-based coatings, *Wear*, **103**(1): 43–55, 1985, https://doi.org/10.1016/0043-1648(85)90121-8.

Received May 16, 2025; revised December 12, 2025; accepted January 14, 2026; available online January 21, 2026; version of record September 9, 2026; published issue XXXX.